International Journal of Advanced Multidisciplinary Research (IJAMR)
ISSN: 2393-8870
www.ijarm.com

Research Article

Theoretical Studies on Mechanism of Xanthine Oxidase and 6-mercaptopurine

Tessema Bashaye Tafesse*

Department of Chemistry, Arba Minch University, Arba Minch, Ethiopia
*Corresponding Author : *bashayetessema@gamil.com*

Keywords

6-mercaptopurine, hypoxanthine, Density functional theory, Hydroxylation, Metastable.

Abstract

The reaction mechanisms of 6-mercaptopurine or hypoxanthine have not been investigated either theoretically or experimentally. Understanding of the overall mechanism helps to manage the metabolic properties of potential drug molecules metabolized by XOR. The present theoretical study is aimed to predict transition state structure, the path of electron transfer and probe plausible mechanistic route for hydroxylation of 6-mercaptopurine or hypoxanthine and XO by relating the electronic structure to reactivity. The transition state structure was predicted by linear transit calculation of series of structures by performing frequency calculation which was confirmed by one imaginary negative frequency value. The path of coupled electron proton transfer mechanism proved from Mullikan charge analysis and mechanism of oxidation was proved from geometry optimization. Density functional theory (DFT)/B3LYP method were used to probe the electronic structure of metastable structure. Result showed that in transition state structures the energy barrier for 6-mercaptopurine bound active site was lower than hypoxanthine bound active site by 20kcal/mol in average. The ionocity data revealed the presence of substantial negative charge on proton which suggests the transfer of hydride from substrate to the active site. Bond length analysis showed that in the transition stases C_{RH}-O_{eq} bond length was nearly 98% formed where as the C_{RH}-H_{RH} bond length was only 36.78% broken. Geometry optimization revealed that oxidation of 6-mercaptopurine or hypoxanthine by XO follow stepwise mechanism. It can be generalized that the oxidation of 6-mercaptopurine or hypoxanthine by XO follows two step mechanisms namely: abstraction of proton by Glu_{1226} from equatorial hydroxide of active site followed by nucleophilic attach on C2 of substrate and hydride was transferred through concomitant release of oxidized substrate.

1.Introduction

1.1 Survey of Molybdenum Enzymes

The oxidation process by molybdenum-containing enzyme, xanthine, is theoretically studied with a model complex representing the reaction center and substrates 6-mercaptopurine or hypoxanthine. The catalytical mechanism for the oxidation of hypoxanthine or 6-mercaptopurine (6-MP) by xanthine oxidoreductase can be studied computationally. The study performed by predicting energy of transition state structures, charge analysis, bond length analysis and from optimization of metastable structures of the reductive half reaction active site xanthine oxidase (XO) bound to 6-mp or hypoxanthine. In all known cases the XO enzymes possess a pterin cofactor, a cofactor required for the activity of enzymes such as sulfite oxidase, xanthine oxidoreductase, and aldehyde oxidase [1, 2]. Enzymes that possess molybdenum in their active sites catalyze biological processes that are essential to the organism; indeed neither plants nor animals can survive without molybdenum [3]. The molybdenum cofactor (Moco) consists of mononuclear molybdenum coordinated by the dithiolene moiety of a family of tricyclic pyranopterin structures, the simplest of which is commonly referred to as molybdopterin [4].

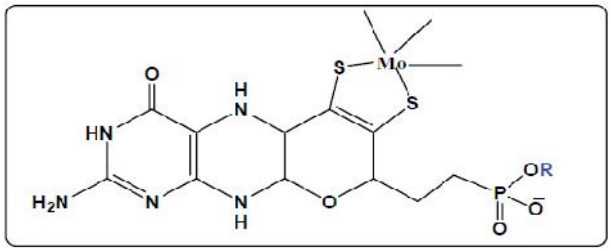

Figure 1.1 Molybdenum cofactor. R=H for eukaryotic enzymes and R=AMP, CMP or GMP for prokaryotic enzymes. Where AMP: - Adenosine monophosphate, CMP:- Cytosine monophosphate, GMP:- Guanine monophosphate [5].

The cofactor modulates the reduction potential of the molybdenum center and facilitates interaction between the molybdenum center and substrate. A significant feature of the molybdenum center is its co-ordination to the cis-dithiolene sulfur atoms that is the only mechanism for fixing the metal to the protein [6].

1.2 The Reaction Mechanism of Xanthine Oxidase Enzyme

Mechanism begins with the extraction of a proton from the hydroxyl of the molybdenum center by Glu_{1261} [18] an event computed to occur readily in the presence of the substrate [8]. The electrons from the deprotonated oxygen are then free to attack the electrophilic C8 atom of the bound xanthine as a substrate. The formation of glutamic acid stabilizes this structure through hydrogen bond interactions [13]. The interactions of Arg_{880} and Glu_{802} appear to vary with analogous substrates and inhibitors, leading to the development of two different modes of substrate binding. One mechanism suggests that Glu_{802} forms hydrogen bond interactions with the C6 carbonyl and N7 of xanthine while Arg_{880} forms hydrogen bonds with the carbonyl of C2 [9]. The second mechanism suggests an inverted orientation of the substrate allowing for hydrogen bond interactions between Arg_{880} and the C6 carbonyl of xanthine. Crystallographic data suggested possible stabilizing interactions between Arg_{880} of the active site and enolate tautomerisation at C6 [18] as shown in figure1.2 below.

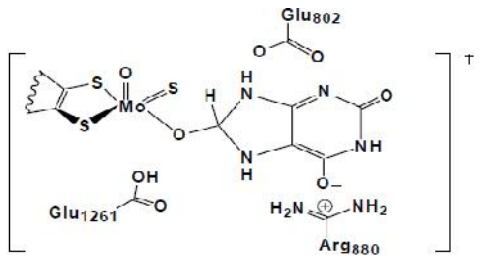

Figure 1.2 Proposed role of amino acid residues (Glue1261, Arg880 and Glu802) for xanthine bound active site XO in transition state. Adapted from reference [18].

Bond formation between the substrate and the molybdenum center orients a Mo=S moiety equatorially to the substrate, positioning it favorably for a concomitant hydride transfer from xanthine [10]. The Mo atom serves as a transducer between the two electrons passed from the substrate to the single electron system of the Fe-S clusters. The transfer of electrons can be monitored through the formation of the paramagnetic transient Mo(V) [10]. Reaction begins by nucleophilic attack of the Mo-OH(H) on the C8 position of substrate, with either discrete formation of a tetrahedral intermediate followed by hydride transfer to the Mo=S group or hydride transfer concomitant with the initiating nucleophilic attack [11].

Currently accepted mechanism of reductive half reaction of xanthine oxidase with physiological substrate xanthine is postulated to take place through a base-assisted nucleophilic reaction [13] as shown in Scheme 1.1.

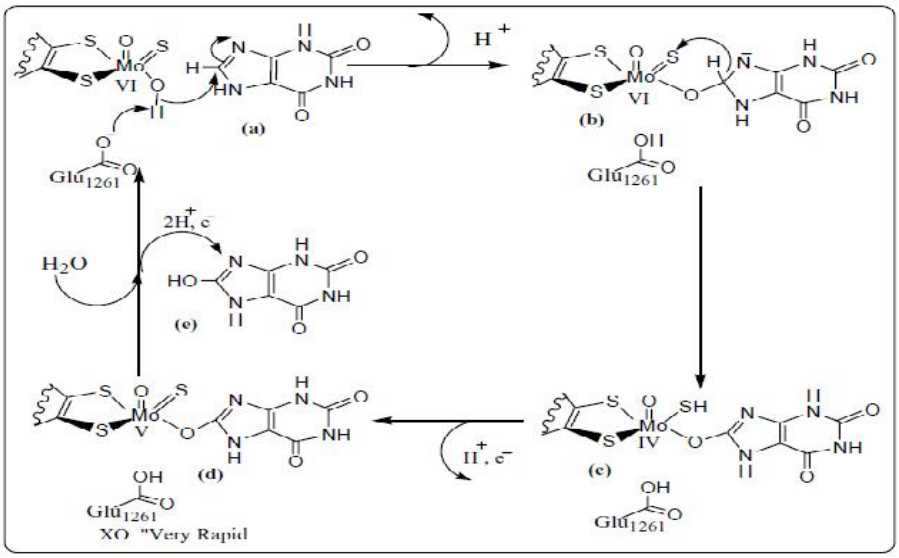

Scheme 1.1 A postulated base-assisted hydride transfer mechanism for the hydroxylation of xanthine by XO enzyme. In the most favorable pathway, the [bm XOR]-Glu_{1261} is proposed to act as a general base. Adapted from reference [15].

Purine substrates hydroxylated at a specific carbon position in a reaction initiated by nucleophilic attack of an equatorial Mo-OH group. Deprotonation is thought to be facilitated by a conserved glutamate residue ($Glue_{1261}$ in the bovine enzyme), as shown in (Scheme 1.1) [7]. Up on nucleophilic attack on substrate carbon (C_{RH}) atom the sp^2 hybridized carbon atom is rehybridized from sp^2 to sp^3 to give tetrahedral complex. The active site pocket itself is lined by several conserved residues: Glu_{802}, Leu_{873}, Arg_{880}, Phe_{914}, Phe_{1009}, and Glu_{1261} [16]. The several hydrophobic residues, Leu_{873}, Phe_{914}, and Phe_{1009}, serve to form the active site pocket [7]. The complete loss of enzymatic activity following mutations of this residue confirms conserved Glu_{1261} has important role in catalysis [7].

1.3 Oxidation of 6-Mercaptopurine and Hypoxanthine

The oxidation of hypoxanthine is theorized to occur much like the oxidation of xanthine. Hence the mechanism begins with the extraction of a proton from the hydroxyl of the molybdenum center by Glu_{1261}. The deprotonated molybdenum oxygen is then free to undergo a nucleophilic attack on C2 of hypoxanthine paired with the concomitant hydride transfer from hypoxanthine to the molybdenum bound sulfido terminal. The study on hypoxanthine shows, it is found in the gas phase as a mixture of two predominant tautomeric forms: the (N1-H, N9-H) and (N1-H, N7-H) keto species. According to the relative stabilities of tautomers, it is suggested that the "bioactive" species corresponds to the (N1-H, N9-H) ketotautomer [14]. Therefore if hypoxanthine replaces xanthine it proceeds through similar reaction mechanism. Chemotherapeutic agent 6-MP and the Physiological substrate hypoxanthine Figure 1.3 below are analogous heterocyclic species. Hypoxanthine is formed by fusing aromatic pyrimidine ring and imidazole to form purine. When 'R' groups of purine derivative, R1=OH and R2=H hypoxanthine is obtained and oxygen on C6 of hypoxanthine is replaced by sulfur 6-MP is formed this implies structurally they have a close similarity.

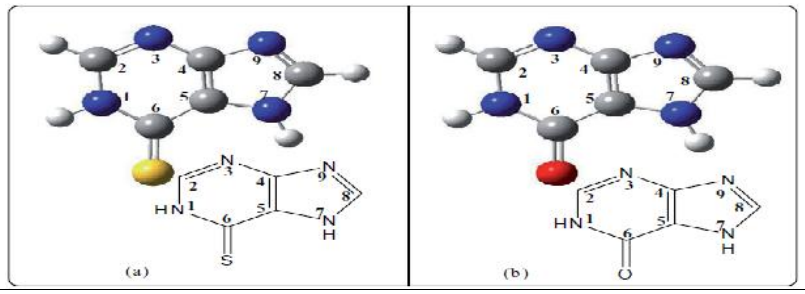

Figure 1.3 Structural analogous of purine (a) 6-mercaptopurine (b) Hypoxanthine (ChemDraw) adapted from reference [13], they are model substrates for this study.

As mentioned above oxidation of hypoxanthine occur much like the oxidation of xanthine then the structural analogue 6-MP will hydroxylated in similar fashion like hypoxanthine. Xanthine have sp^2 hybridized electrophilic carbon that hydroxylated by xanthine oxidase. Hypoxanthine and 6-MP also has sp^2 hybridized electrophilic carbon. Therefore if xanthine is replaced by hypoxanthine or 6-MP they undergo similar reaction with xanthine oxidase but expected to passes through different intermediate as shown in Scheme 1.2.

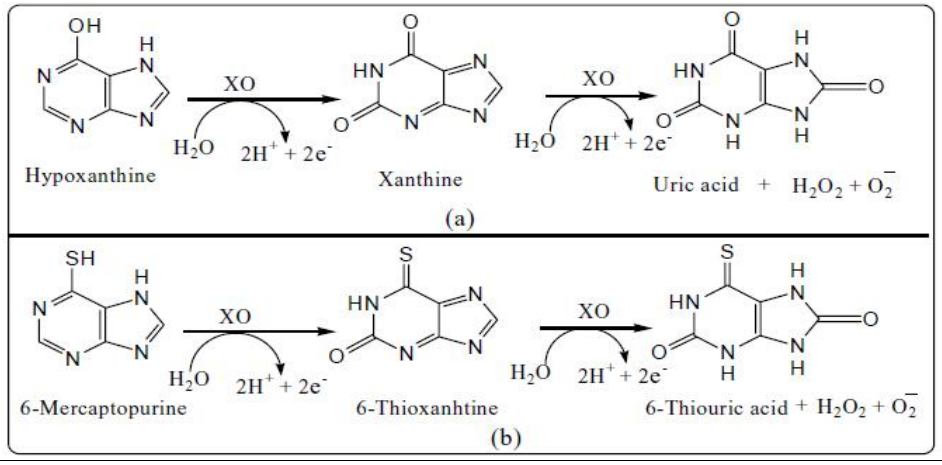

Scheme 1.2 (a) Oxidative hydroxylation of hypoxanthine to xanthine and xanthine to uric acid, (b) Oxidative hydroxylation of 6-mercapto purine to 6-thioxanthine to 6-thiouric acid and (b). Adapted from reference [17].

Physiological substrate hypoxanthine and the chemotherapeutic agent 6-MP have two alternate orientations in the active sites. Due to the presence of two carbons (C2 and C8) sp^2 hybridized electrophilic carbons. Crystal structure shows that both the overall orientations of substrate and positions of the several active site amino acids are very similar for hypoxanthine and 6-mercaptopurine, except that Thr_{1010} appears to hydrogen bond to N1 or N7 (for the orientations with C2 and C8 proximal, respectively) of hypoxanthine but not to 6-MP. This appears due to a rotation of 6-MP by approximately 15° to accommodate the larger sulfur atom at the C6 position [34]. Both orientations have exocyclic functional group at the C6 position adjacent to a conserved arginine (Arg_{880}) residue. The formation of C6 -O- and C6 -S- during the transition state better stabilized through the interaction with the positively charged arginine (Arg_{880}) [18]. It is already discussed that hypoxanthine hydroxylated in similar way as xanthine in addition Hypoxanthine and 6-MP are structurally similar. Furthermore they all have sp^2 hybridized electrophilic carbon and hence it is expected that hypoxanthine or 6-MP follow similar hydroxylation rout as like as xanthin. The binding stage from the currently accepted general mechanism proceeds through nucleophilic attack by active site on C8 of xanthine to form tetrahedral complex as shown in scheme 1.3.

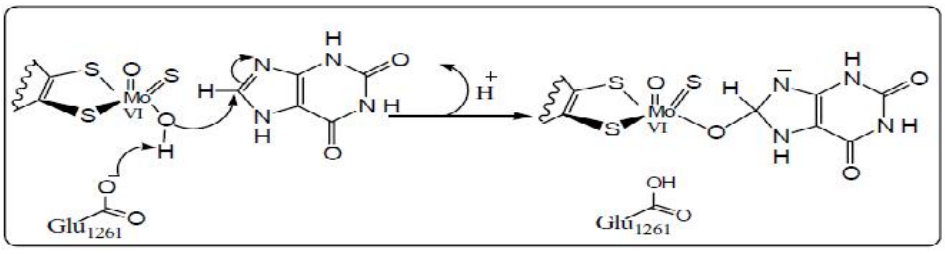

Scheme 1.3 Currently accepted reaction mechanism for binding stage of xanthine bound active site xanthine oxidase.

The binding stage for 6-mercaptopurine or hypoxanthine can be represented similarly as Scheme 1.4 above.

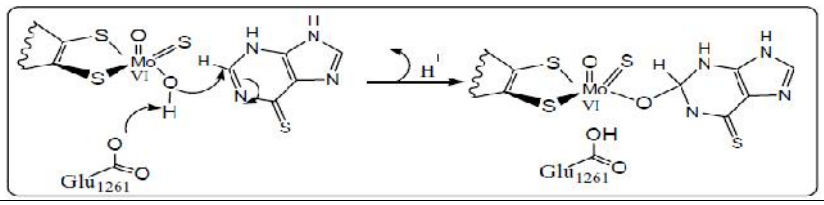

Scheme 1.4 Proposed reaction mechanism for binding stage of 6-mercaptopurine or hypoxanthine bound active site xanthine Oxidase.

Therefore from Scheme 1.1 and 1.4 it can be concluded that tetrahedral complex could be formed in the binding stage of all xanthine, hypoxanthine and 6-MP. Four routes may be proposed through which the hydroxylation of 6-MP or hypoxanthine proceeds Scheme 1.5.

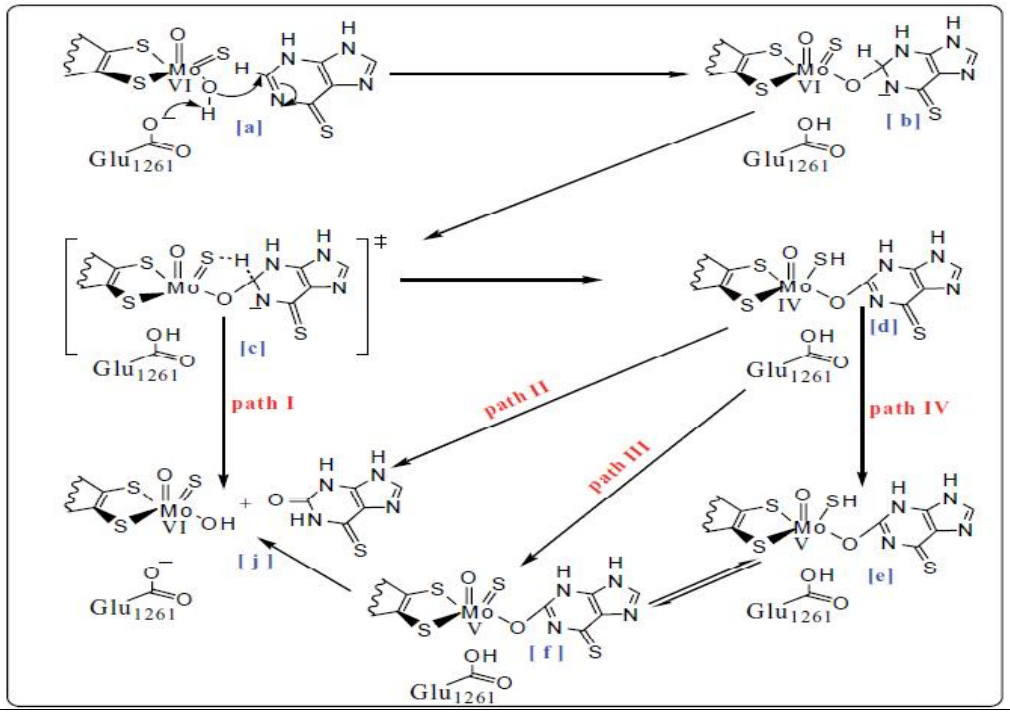

Scheme 1.5 Hypothetical schematic model for the catalytic transformation of oxidation and hydroxylation of 6-mercaptopurine or hypoxanthine by XO enzyme.

2. Materials and Methods

2.1 Materials

Structures were developed using GaussView 3.0 and CS Chem3D pro 1999 (Cambridge Soft Corp., Cambridge, MA, U.S.A.). All Calculations were performed using Gaussian 03W (version 6.0) program software package (Gaussian, Inc., Wallingford, CT, U.S.A.). The inputs were prepared for submission to Gaussian and to examine graphically the output of (Optimized molecular structures, molecular orbital, atomic charges, and animation of normal model corresponding to vibrational frequencies) and other Gaussian products were visualized using software programs such as GaussView 3.0 (Gaussian, Inc., Pittsburgh, PA, U.S.A.).

2.2 Methods

Density functional theory (DFT) was applied to optimize the structures. Becke's three- parameter exchange function and the Lee, Yang and Parr correlation functional (B3LYP) method were employed in the DFT calculations. The 6-31G (d', p') basis set with a polarization function was used for non-metal atoms (C, H, O, N, and S). Similarly, LANL2DZ (Los Alamos National Laboratory 2 Double Zeta) effective core potential (ECP) basis sets were used for Mo atoms.

2.2.1 Predicting the transition state structures

The general structure shown in Figure 1.4 was used to predict the transition state structures. The substrate (C_{RH}) in Figure 1.4 was replaced by 6-MP or hypoxanthine with up and down conformations. The transition state was determined by linear transit calculation through linear motion of hydrogen bound substrate (H_{RH}) during the migration of hydrogen (H_{RH}) from substrate (C_{RH}) C2 to sulfide terminal (Mo=S) of xanthine oxidase. The transition state structures were characterized by:- transition state energies, Frequency calculation, Mullikan charge and bond length analysis.

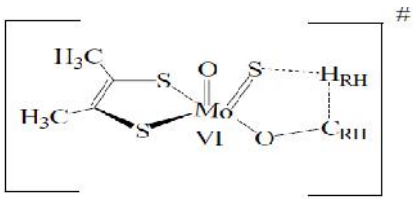

Figure 1.4 A general structure for the transition state.

The geometries were modeled in (a) N-up (b) N-down, (c) N-down, and (d) N-up conformations. N-up and down, represents the negative charge on N3 is above and on N1 is below the equatorial plane of 6-mercaptopurine or hypoxanthine bound truncated Moco.

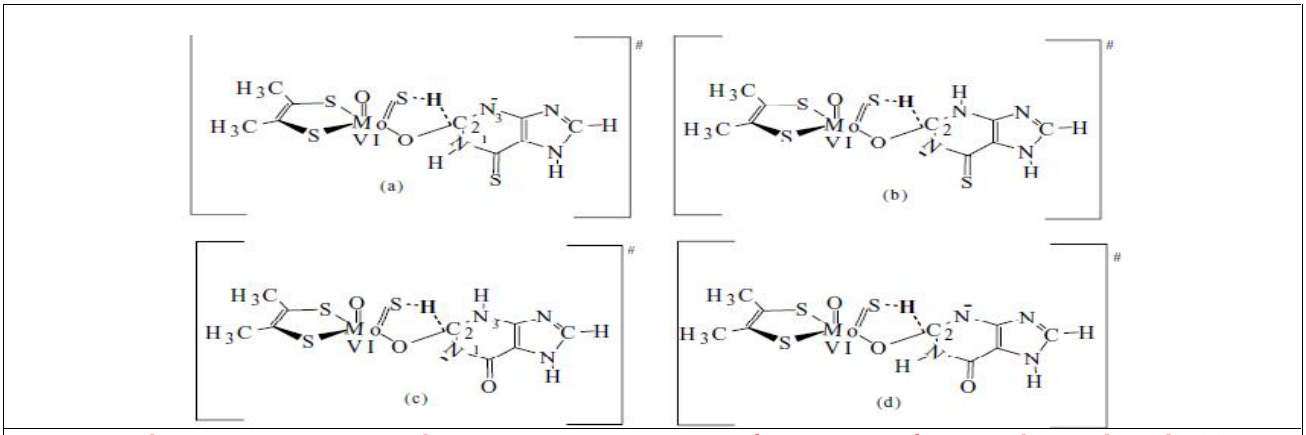

Fig 1.5 The geometries represent the transition state structures of MoVI state of truncated Moco bound:- (a) 6-mercaptopurine up, (b) 6-mercaptopurine down (c) hypoxanthine down and (d) hypoxanthine up.

The output of Gaussian was viewed using GaussView; then Mullikan atomic charge, bond distance and energy of the optimized structure were collected. The same procedure was followed for all other linear transit calculations of the substrates bound truncated active site.

2.2.2 Geometry Optimization

From the linear transit calculation transition state energy were taken and optimization of Reactants (6-MP, hypoxanthine, and active site xanthine oxidase), products (6-Mo(VI)(b), Mo(IV)(d) and EPR reactive complex Mo(V)(e) and (f) of reductive half reaction active site bound 6-MP or hypoxanthine were also optimized as shown in hypothetical schematic model given below Scheme 1.6. The energy from linear transit calculation and from geometry optimizations provide complete energy level diagram.

Comparisons of concerted and stepwise path were performed to develop the plausible mechanism through which the reaction proceeds. Below four paths were proposed for the oxidation of substrate (C_{RH}) by xanthine oxidase. The energies of the output from the geometry optimization versus S_{Mo}-H_{RH} distance for all four possible paths plotted and the energies were compared. The path which utilized lowest energy was considered as the mechanistic route through which the oxidation of substrate (C_{RH}) by xanthine oxidase proceeds. The same geometry optimizations routs were followed for hypoxanthine and 6-mercaptopurine to determine the mechanism of reaction.

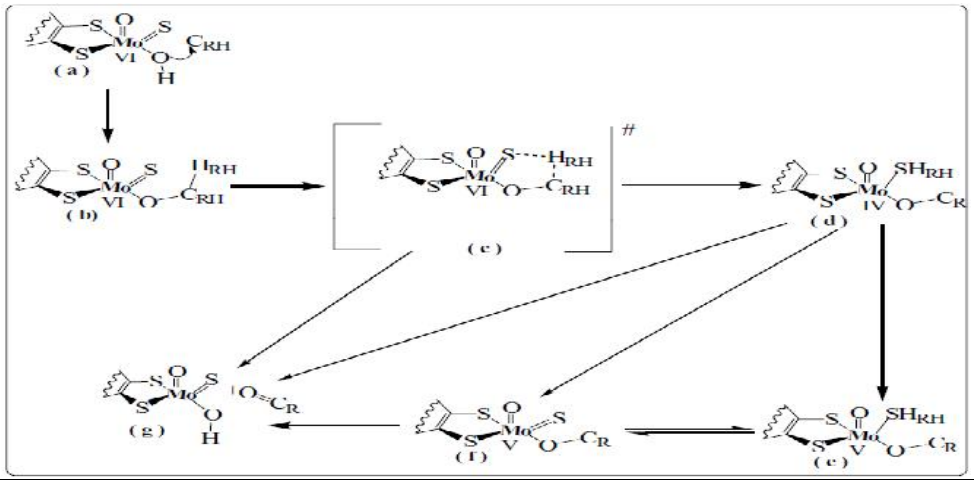

Scheme 1.6 A hypothetical general schematic model for the catalytic transformation of the oxidation of substrates (C_{RH}) by XO enzymes proceeds through either concerted or stepwise reaction mechanism.

3. Results and Discussion

3.1 Predicting Transition State Structure

Linear transit energy difference plots between 6-mercaptopurine up and down

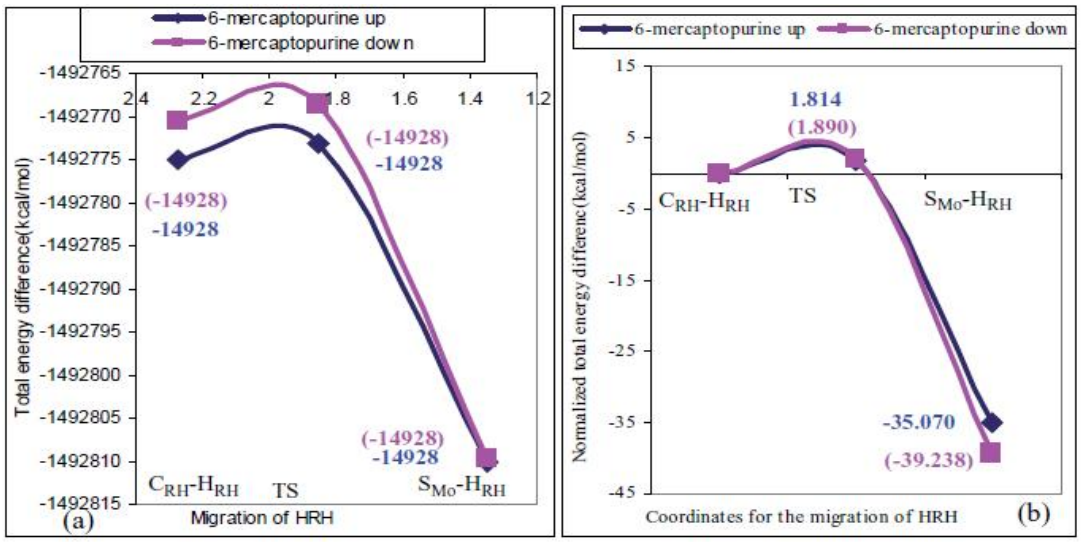

Figure 1.5 (a) Linear transit total energy difference of 6-mp up and down conformers for migration of H_{RH} from C_{RH}-H_{RH} to SMo-H_{RH} through TS. (b) Normalized total energy, where C_{RH}-H_{RH}: - energy differences when hydrogen is bound to C2 of substrate, TS: - Energy differences when active site bound substrate is at transition state and SMo-H_{RH}: - energy difference when the active site is in a reduced state as Mo (IV). Plot (a) the trace from top to bottom of left side designate: - 6-mp down (1st trace or pink color) and 6-mp up (2nd trace or dark blue color). Plot (b) the trace from top to bottom of right side:- 6-mp up (first trace or dark blue) and 6-mp down (2nd trace or pink color). The energy values for 6-mp down are given in parenthesis and for 6-mp up are without parenthesis. The plots were developed from the raw data Table A.1.1 (Appendices)

From the transition state energy at S_{Mo}-H_{RH} distance (1.85104Å) 6-MP up < 6-MP down < hypoxanthine up < hypoxanthine down. In transition state 6-MP up bound the reductive half reaction active site is stabilized by 4.55kcal/mol and that of hypoxanthine up bound the reductive half reaction active site is stabilized by 7.131kcal/mol relative to the down conformers.

Linear transit energy difference plots between Hypoxanthine up and down

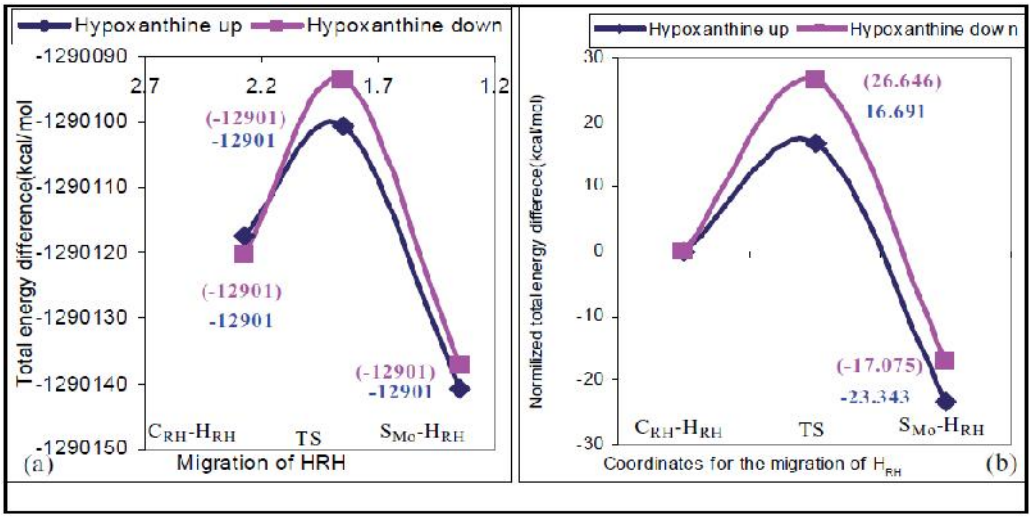

Figure 1.6 (a) Linear transit total energy difference for Hypoxanthine up and down conformers. (b) Normalized energy. Where C_{RH}-H_{RH}: - energy differences when hydrogen is bound to C2 of substrate, TS: - Energy differences when active site bound substrates are at transition state and SMo-H_{RH}: - energy difference when the active site is in reduced state as Mo (IV). Plot (a) the trace from top to bottom of right side: - hypoxanthine down (first trace or pink color) and Hypoxanthine up (second trace or dark blue). Plot (b) the trace from top to bottom of right side: - hypoxanthine down (first trace or pink color) and Hypoxanthine up (second trace or dark blue). The energy values for hypoxanthine down are given in parenthesis and for hypoxanthine up are without parenthesis. The plots were developed from the raw data Table A.1.1 (Appendices)

The difference of normalized total transition state energy of the two substrates 6-MP and hypoxanthine up and down conformers is 14.878kcal/mol and 24.755kcal/mol respectively. Therefore from transition state energy it can be concluded that the up conformers require lesser energy for its transformation to the transition state.

Frequency values of transition states

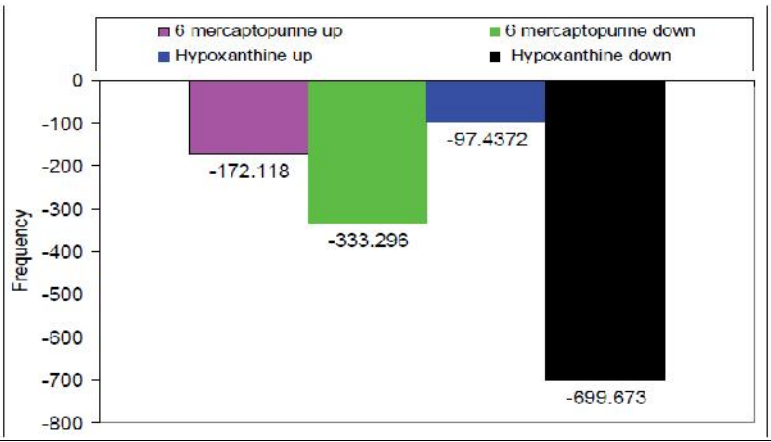

Figure 1.7 Calculated frequency values 6-mp and hypoxanthine. From left to right 6-mp up (first bar or pink color), 6-mp down (second bar or bright green color), hypoxanthine up (third bar or blue color) and hypoxanthine down (fourth bar or black color). The graphs were developed from the data Table A.1.1 (Appendices).

The frequency of up conformer is greater than the down conformer by 161.178 and 602.2358kcal/mol for 6-MP and hypoxanthine respectively. Therefore the frequency of vibration of up conformer is expected to be greater than the down conformers hence the higher the rate of decomposition of the transition state structure.

The Mullikan atomic charge distribution for the interaction sites of substrates.

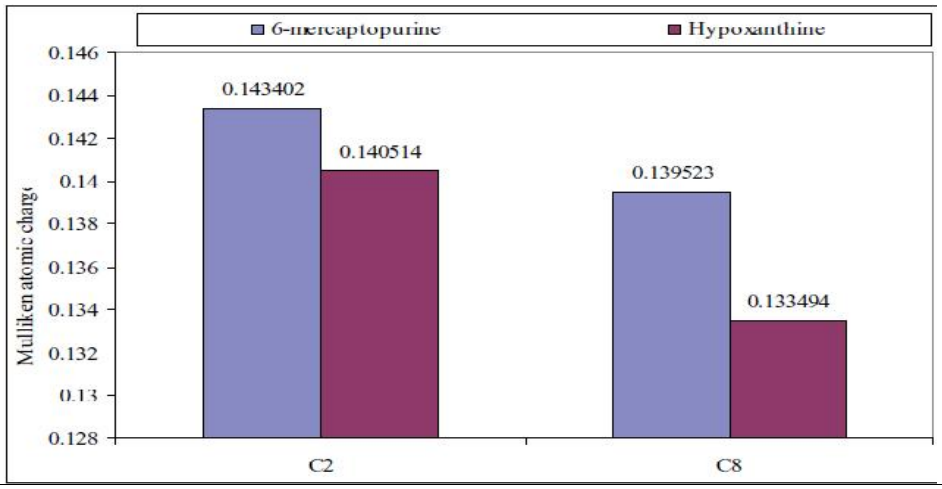

Figure 1.8 The Mullikan atomic charges difference between 6-mp and hypoxanthine. The bar graphs containing C8 and C2 represent 6-mp (left side) and hypoxanthine (right side) from each of the two bars. Substrates are 6-mp (C8: carbon in the eighth position, C2: carbon in the second position). The same designation was used for Hypoxanthine. The graphs were developed from the raw data of the optimized substrates given in Table A.1.4 (Appendices).

Path of Electron Transfer

The Mullikan atomic charge of Mo of substrate bound active site is (0.624793), in the transition state it is (0.391551) decreased by (0.233242), still it is electropositive with value ranging from 0.624793 to 0.398834 as compared to other coordinated atom showing its metallic character normalized Mullikan charge. No change is observed after transition. The change in Mullikan charge of Mo indicates the accumulation of charge in its reduced state Mo(IV) in the reductive half reaction which is oxidized to Mo(VI) up on oxidative half reaction. The Mullikan population of electrophilic C2 of substrate (C_{RH}) bound equatorial oxygen of active site is (0.29105), in the transition state it is (0.45237) increased by (0.16132). The Mullikan charge for carbon increased or become more positive as Oeq approaches and H_{RH} migrates away for normalized charge density. This may be due to removal of electron as hydride transferred toward sulfido terminal. The hydride transfer from substrate C2 to sulfido terminal was supported by a number of studies [21]. The Mullikan atomic charge for hydrogen bound C2 of substrate (H_{RH}) is (0.073131) in C_{RH}-H_{RH} and it is (-0.07357) in the transition state, decreased by (0.146701) that is around two fold increase in electron density. Gradually the negative charge decreased to (-0.0107) as it bound to the terminal sulfido (S_{Mo}-H_{RH}).

Equatorial oxygen (O_{eq}) of active site at the beginning is (-0.55619), in transition state its charge is (-0.44026), decrease the electron density by (0.11593) and again decreased to (-0.43539) when it bound to C2 of substrate. The charge density for equatorial oxygen decreased or become less electronegative as it moves from active site to substrate hence the possibility of electron transfer from substrate to active site through equatorial oxygen, orthogonal proton coupled electron transfer may be ruled out. Apical oxo (Mo=O) showed no significant change in Mullikan atomic charge relative to other atoms as it form a straight trace for the migration of H_{RH}. Decreased from (-0.50465) to (-0.51647) by (0.01182). The Mullikan atomic population of Oxo group (Mo=O) is (-0.50465), that of equatorial oxygen (O_{eq}) is (-0.55619), O_{eq} negative than oxo group by (0.05154).

Even if the difference is not so large it can be concluded that O_{eq} is a better nucleophile for its higher negative charge. Therefore the catalytically labile site should be the metal-coordinated hydroxide (O_{eq}) rather than the apical oxo group (Mo=O). This is consistence with theoretical study [20] and in addition to its less electronegativity; the X-ray structure analysis showed that lack of enough space for the substrate to approach the Mo center from the axial direction [12] other factor which may decrease its reactivity. The Mullikan atomic charge of terminal sulfido

(S_{Mo}) is (-0.46586) for substrate bound active site, in the transition state it is (-0.34216) decreased or become less electronegative by (0.1237) and finally when S_{Mo} bound hydrogen (H_{RH}) of substrate it is increased to (-0.36711).

The charge of dithiolene sulfurs, sulfur back (S_{back}) for substrate bound active site is (-0.14252), at transition state decreased to (-0.1899) by (0.04731) and finally decreased or become more electronegative to (-0.20266) as H_{RH} bound S_{Mo}. The charge of sulfur front (S_{front}) at the beginning is (-0.14187), at transition state decreased to (-0.21479) by (0.07292) and finally decreased or become more electronegative to (-0.2233) as H_{RH} bound S_{Mo}. The decrease in charge is larger for sulfur front (S-front) by (0.08143) as H_{RH} migrates from C_{RH} to S_{Mo} than S-back which is decreased by (0.06014) and S_{front} greater than S_{back} by (0.02064); this is probably back bonding of metal in plane d_{xy} orbital with sulfur out of plane p_z orbitals which may delocalize electron between S-back and Mo. The electron density of S_{back} may favored towards Mo in order to induce oxygen transfer and modulate electron density on oxidized and reduced forms of active site, this explains the influence of trans effect S_{back} to facilitate O_{eq} transfer, where as S_{front} experience less synergic effect as it cis to O_{eq}. In general the increase in electronegativity may be attributed by the increase of electron densities on dithiolate sulfur (-0.2233 & -0.20266) S-front and S-back respectively which facilitate the movement of equatorial hydroxide towards C2 of substrates (C_{RH}). It was indicated by the study of fold angle of dithiolate density at the metal center [20].

There are two possible interaction sites of substrate at the active sit C2 and C8. A DFT calculation of charge distribution for 6-MP is (0.143402 and 0.139523) on C2 & C8 respectively. That of hypoxanthine is (0.140514 and 0.133494) on C2 & C8 respectively. The Mullikan atomic charge of hydrogen atoms (H_{RH}) boundC2 of 6-MP and hypoxanthine is (0.171649 and 0.15786) and bound C8 is (0.08821 and 0.080245) respectively. Hydrogen on C2 is labile for hydride transfer due to its electronegative nature for 6-MP or hypoxanthine. Both these factors indicate that the C2 position is more susceptible to nucleophilic attack by hydroxide of active site. Electrophilicity of C2 of 6-MP is greater than hypoxanthine, this implies the interactive site of 6-MP is reactive for nucleophilic attack relative to hypoxanthine. In support of interactive site the study of sequential hydroxylation of hypoxanthine indicated that hypoxanthine is hydroxylated exclusively at the C2 position and C2 of hypoxanthine is comparably reactive as C8 of xanthine [18].

Bond length change for the migration of H_{RH} from substrate to sulfido terminal S_{Mo}.

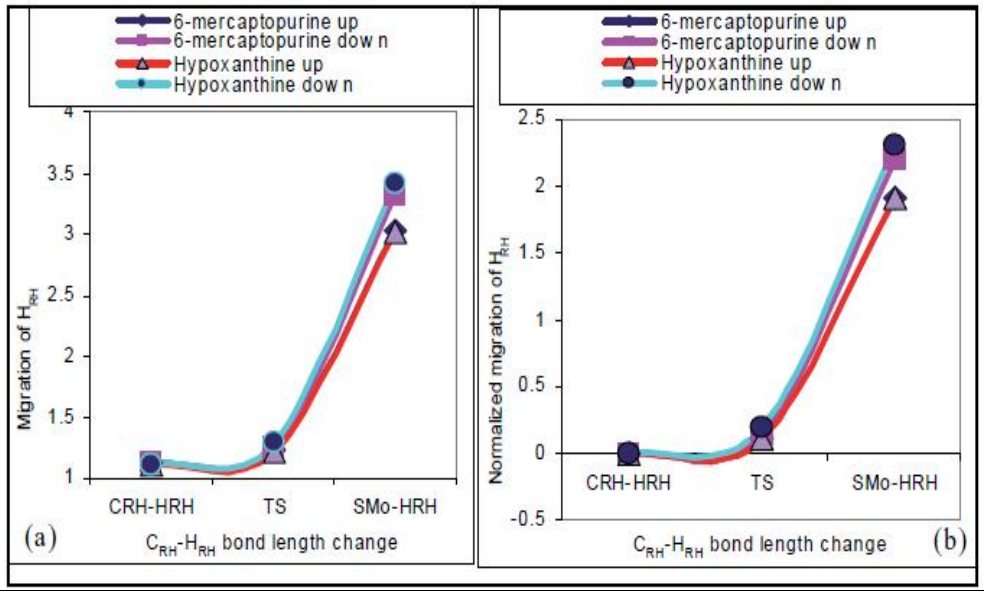

Figure 1.9 Linear transit bond length trend for the migration hydrogen (H_{RH}) from the carbon (C_{HR}) to sulfido terminal (S_{Mo}). Plot (b) represents normalized bond length. The traces for hypoxanthine and 6-mp conformers are overlapped together. In both case the right upper trace is hypoxanthine and the right lower trace represents 6-mp. The plots were developed from the raw data Table A.1.3 (Appendices).

Bond length change for the migration of O_{eq} from enzyme to substrate carbon.

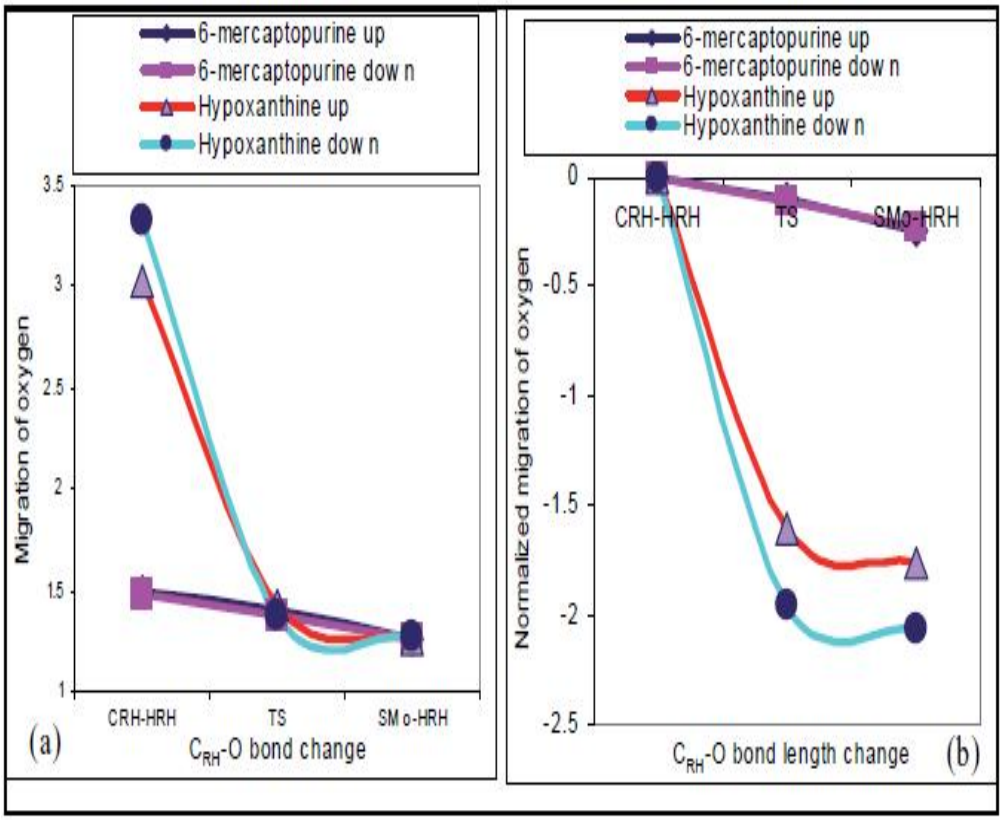

Figure 1.10 Linear transit bond length plot for the migration oxygen from molybdenum site of terminal hydroxide (Mo-OH) to substrate C2. Plot (b) is for normalized bond length. Plot (a) the traces from top to bottom from the left side: - Hypoxanthine down (1st trace or turquoise color), Hypoxanthine up (2nd trace or red color) and 6-mp up and down already overlapped each other (third trace). Plot (b) the traces from bottom to top in the right side: - Hypoxanthine down (1st trace or turquoise color), Hypoxanthine up (2nd trace or red color) and 6-mp up and down already overlapped each other (3rd trace). The plots were developed from the raw data Table A.1.3 (Appendices).

In the transition state the Mo-OH bond distance lengthens from 1.9212Å to 2.1806Å increased by 0.2594Å and it is about 79.84% broken relative to reactant geometry (1.74108 Å). The C_{RH}-Oeq bond distance shorten from 1.49178Å to 1.2578Å decrease by 0.23398 Å and it is about 98% formed relative to product geometry (H_{RH}-C_{RH} bond length 1.23287Å) differ from product C_{RH}-O_{eq} bond length by 0.02493Å . Also the C_{RH}-H_{RH} distance lengthens from 1.12405Å to 2.99513Å increased by 1.87108Å which is indicated by positive gradient and about 36.78% is broken relative to reactant geometry (1.10167Å), while the H_{RH}-S_{Mo} bond distance decreased from 2.27427Å to 1.74612Å shorten by 0.52815Å . The shortening of C_{RH}-Oeq bond length helpful to build up sufficient electron density which support hydride transfer. The bond lengths o f dithiolate sulfur of Mo-S_{front} shorten from 2.5111Å to 2.4366Å decreased by 0.0745Å and Mo-S_{back} bond length changed from 2.522Å to 2.4153Å shorten by 0.1067Å. The bond length of Mo-S_{back} decreased by a factor 1.43 relative to Mo-S_{front} bond length. This may be due to significant back donation of electron from molybdenum to S_{back} as compared to S_{front}. The increase electron density between Mo and S_{back} facilitate the transfer of equatorial oxygen towards C2 of substrate (C_{RH}). On the other hand S_{back} is the atom trans to the leaving group (O_{eq}) and is responsible to push O_{eq} by accumulation of electron density on the metal center which agree with the trans effect theory to which the ligand weaken the bond trans to itself

.

3.2 Geometry Optimization

Energy plot from geometry optimization for each path

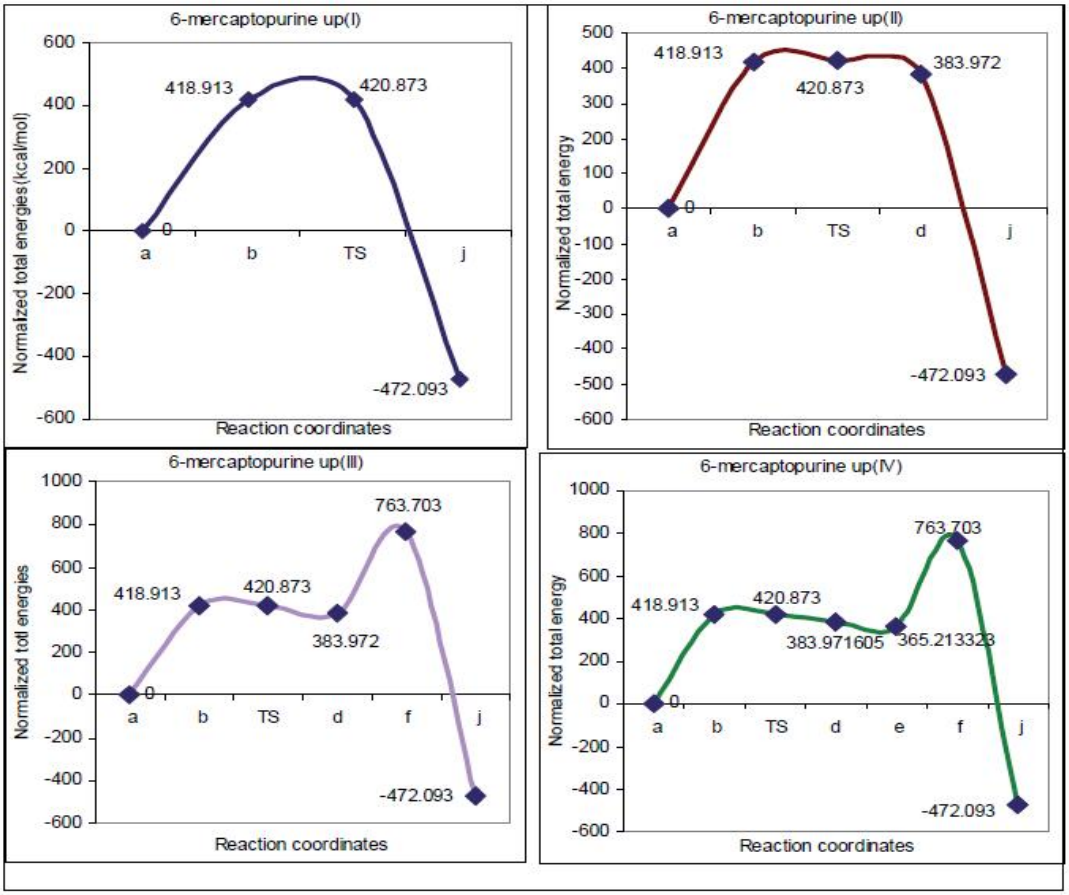

Figure 1.11. The total energy plots from geometry optimization. The four paths were separately given. 6-mercaptopurine (I) represent for path I, 6-mercaptopurine (II) represents path II and so on. The plots were developed from the raw data Table A.1.5 (Appendices).

The geometrical features for bond length in transition state suggest that C_{RH}-O_{eq} bond formation is nearly complete in the transition state and that of C_{RH}-H_{RH} broken to smaller extent. The shortening of C_{RH}-O_{eq} bond increases electron density on carbon atom which contributes for inducing hydride transfer. Hence the reaction is dominated by the nucleophilic addition since almost the C_{RH}-O_{eq} bond nearly completely formed relative to C_{RH}-H_{RH} bond which is about 37% broken. It is consistence with result obtained for the theoretical study of oxidation of xanthine oxidase with formamide [8]. The nucleophilic attack forms tetrahedral intermediate followed by hydride transfer, therefore hydride transfer is the rate determining step for the reaction since it the slowest step. Also the bond length of Mo=S increased from 2.22188Å to 2.40494Å elongated by 0.18306Å which implies the loss of the double bond character. This may be due the presence of electron delocalization between Mo and sulfido terminal. Therefore it is assumed that the electron form the substrate to the active site is transferred through sulfido terminal. In support of this, study showed that sulfido terminal is equatorial location appropriately positions the Mo=S ligand to accept a hydride ion from the reactive carbon atom to produce Mo-SH and a reduced molybdenum center [22]. As it was discussed previously that catalytical center of reductive half reaction active site bound substrate are Hydrogen (H_{RH}) atom bound C2 of substrate and terminal sulfido bound molybdenum (S_{Mo}). The subsequent hydride attack on the sulfur atom will weaken the Mo=S double bond by populating the orbital and thus ease the formation of a sulfhydryl group (Mo-SH), a crucial enzymatic step [21] also supports this idea. Consequently, the level of separation between LUMO of active site and HOMO of substrate decreased which facilitates the hydride transfer to form sulfhydryl group. The two-electron transfer from substrate was induced through incorporation of an oxygen atom into substrate.

The lowest unoccupied molecular orbital, LUMO which has antibonding character between the sulfido and empty d_{xy} Mo orbital is derived from the highest occupied molecular orbital after it accepted two electrons from HOMO of substrate was discussed by studies of other model complexes of aldehyde oxidase reductive half reaction [20]. The dithiolate involves in strong mixing with an empty metal d_{xy} orbital when the electron density in the metal orbital is low, for oxidized Mo (VI). The dithiolate also involve themselves by localization of electron density on the sulfur- orbitals in the presence of high electron density on the metal orbital in reduced Mo (IV).

Hence during such overlap it is expected that the contributions from the dithiolate increases in the redox reaction with concomitant decrease in the metal contribution.

Mechanism of reactions

For reaction mechanism the up conformers were selected depending on the minimum energy barrier they required for the transformation from reactant to transition state. Four paths were proposed through which the reaction may proceed: path I, path II, III, and IV as shown in Scheme 1.5. Analysis of path IV and path III implies that the energy barrier between transition state and complex [f] (Scheme 1.6) is about 342.83kcal/mol which is very large relative to path I and II. The reaction cannot proceed through these two paths having high energy barrier hence path III and IV can be ruled out. Path II has 36.9kcal/mol energy barriers between transition state and product bound active site structure [d] relative to path I which indicates the hydroxylation reaction was not expected to take place through path II. Therefore path II, path III and IV would display retardation of product formation by 36.9kcal/mol, 342.83kcal/mol and 342.83kcal/mol relative to path I considering the energy difference between transition state and the highest energy they have on path. In path I and II a tetrahedral intermediate was not observed where as path III and IV passes through a tetrahedral product bound intermediate.

Energy barrier observed in path II, III and IV are not found in path I therefore our focus is examining path I which proceeds product formation with minimum energy. For path I there is no energy barrier after transition state and the transition state decompose to products so easily due to very large exothermic value of the product releasing step which extremely thermodynamic product. The calculated energy barrier between reactants (6-MP or hypoxanthine and active site) and substrate bound active site for path I was about 420.87kcal/mol which is so large. In theoretical studies on the mechanism of aldehyde oxidase and xanthine oxidase a higher barrier of 40kcal/mol was reported from a pre-association complex that is not on the reaction pathway. This pre-association complex is unlikely to form in the enzyme active-site [8]. But in our case the energy barrier is so large hence cannot be considered as pre-association energy. This large energy indicates the presence of other high energy species and or intermediate. The species may be transition state structure between the reactant and the substrate bound active site intermediate.

Hence it is suggested that the abstraction of proton from hydroxide ligand of active site by Glu_{1261} and simultaneous nucleophilic attack of hydroxo group on C2 of substrate coexist in the transition state. Hence the reaction may possess two transition state (TS1 and TS2), the first step is the abstraction of proton from the hydroxide ligand by Glu_{1261}; concomitantly nucleophilic attack on C2 of substrate to produce substrate bound active site as intermediate (INT) Scheme 1.7. This process takes place through transition state TS1.

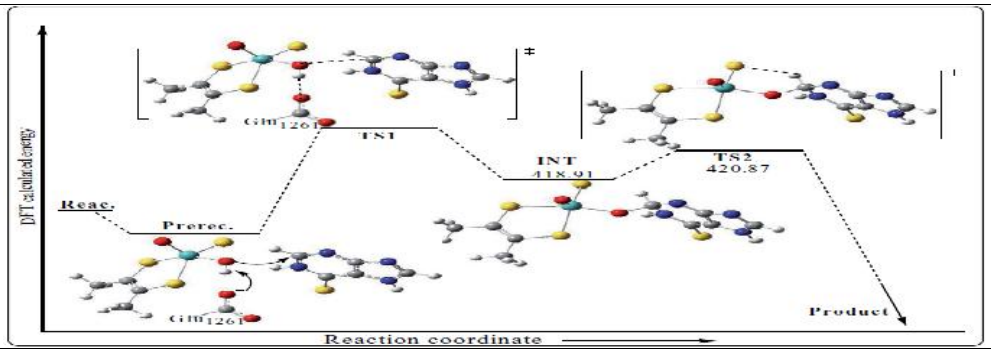

Figure 1.12 Energy diagram for the conversation of 6-mercaptopurine to 6-thiouric acid. The total energy change for the reaction mechanism of oxidation of 6-mercaptopurine or hypoxanthine by xanthine oxidase contains five reaction stages: Reac. :-Infinitely separated reactants, Prerec. :-Pre-association interaction [improved pre-association reaction], TS1:- transition state one [expected transition state interaction], INT: - intermediate, TS2:- transition state two and product: - product release stage at which 6-thiouric acid or uric acid infinitely separated from active site [the arrow in the represents for very large exothermic reaction product (-1540416.156) kcal/mol and (-1337752.554) kcal/mol for 6-mercaptopurine and hypoxanthine respectively].

The Mullikan population of H_{RH} in INT is 0.075993, in TS2 it decreased to 0.04938, and gradually converted to -0.07357 change by 0.149563. The conversion of H_{RH} from 0.075993 to -0.07357 indicates the density of charge increased as the reaction proceed from INT through TS2 to product bound complex. Relatively Mullikan population of H_{RH} for free substrate 6-MP is 0.171649 and in the INT decreased by 0.095656. If there were no transition state the change in charge of H_{RH} will be insignificant. This implies a significant change of the charge of H_{RH} was observed in TS1. In the course of the reaction two electrons and a proton are transferred from the substrate to the molybdenum center followed by dissociation of hydroxylated product. The most important feature for the enzymatic reaction considered is a hydride transfer from the substrate to the sulfido group of Mo. The barrier for proposed TS1 and INT is expected to be greater due to proton abstraction step; relatively the energy barrier between the INT and TS2 is about 2kcal/mol implying that the transformation of INT to TS2 of hydride attack step require lesser energy. The expected proton abstraction by Glu_{1261} to produce INT is rate determining step. Once TS2 is formed the product released very rapidly due to very large energy was released as the reaction proceeds from TS2 to product formation.

Hence it was proposed that hydroxylation of 6-MP or hypoxanthine by xanthine oxidase proceeds through stepwise mechanism. In TS1 Glu_{1261} and 6-MP or hypoxanthine bound active site coexists together. From TS1 substrate bound active site intermediate INT is formed followed by TS2 formation. The second transition TS2 is the usual hydride transfer from substrate to sulfido terminal followed by release of hydroxylated product. Based on the above hypothesis the following general mechanism for the hydroxylation of 6-MP or hypoxanthine by xanthine oxidase was probed as shown in Scheme 1.7.

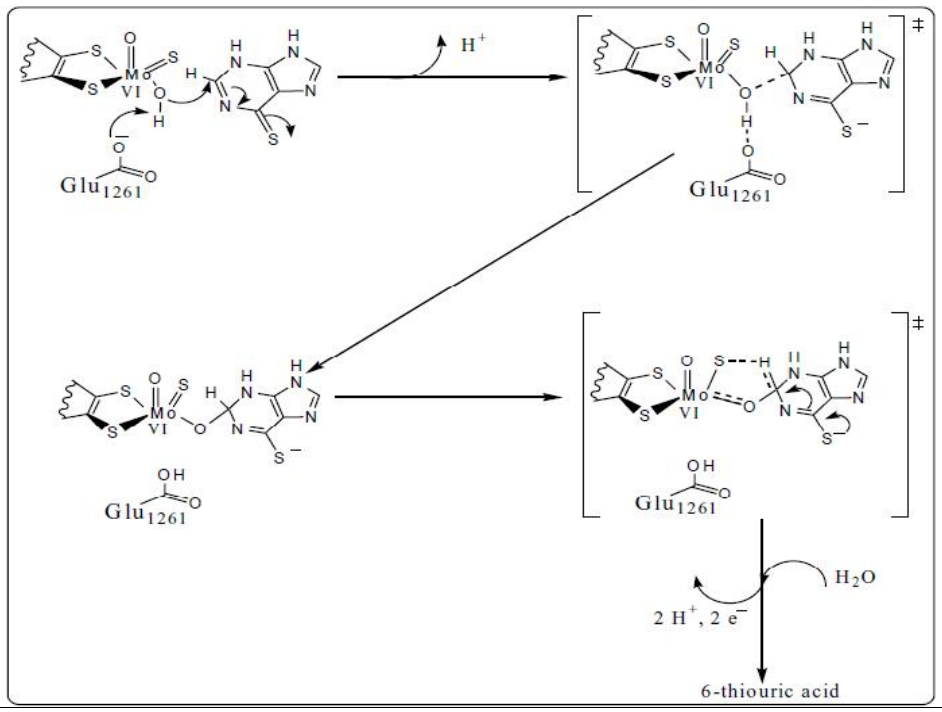

Scheme 1.7 Proposed mechanism for the hydroxylation of 6-mercaptopurine by xanthine oxidase enzyme. The hydroxylation reaction at the C2 position of 6-mercaptopurine is initiated by abstraction of proton by Glue1261 followed by nucleophilic attack of Mo –O- to give the reaction intermediate (INT) through transition state (TS1). The intermediate (INT) then undergoes hydride attack followed by release of hydroxylated product through (TS2). Hydroxylation reaction at the C2 position of hypoxanthine occurs in the same way as in the case of the 6-mercaptopurine.

4. Conclusion

The amino acid that plays an important role in the catalytic reaction is Glu_{1261}. Including Glu_{1261} other active site amino acid residues Arg_{880} and Glu_{802} play an important role in the mechanism of reaction. The reaction catalyzed by hydride transfer from the sp^2 carbon of substrate to the active site sulfido terminal. The hydride transfer from substrate C2 to sulfido terminal was supported by a number of studies [10]. The charge density on equatorial oxygen (O_{eq}) decreased by (0.11593) and hence the possibility of electron transfer from substrate to active site

through equatorial oxygen, or orthogonal proton coupled electron transfer may be ruled out. Apical oxo (Mo=O) showed no significant change in Mullikan atomic charge relative to other atoms implying that it has no significant contribution for catalytic reactions. The charge of equatorial oxygen (Oeq) is (-0.55619), it is more negative than apical oxo group by (0.05154). Therefore the catalytically labile site should be the metal-coordinated hydroxide (Oeq) rather than the apical oxo (Mo=O) for nucleophilic attack. In addition to its less electronegativity X-ray structure analysis showed that lack of enough space for the substrate to approach the Mo center from the axial direction [12]. In the transition state the Mo-OH bond distance increased by 0.2594Å. The C_{RH}-O_{eq} bond distance decrease by 0.23398Å and it is about 98% formed relative to product geometry and hence the reaction was dominated by nucleophilic attack which is consistence with result obtained for the theoretical study of oxidation of xanthine oxidase with formamide [19]. Also the C_{RH}-H_{RH} distance lengthens and about 36.78% is broken relative to reactant geometry and hence hydride transfer is the rate determining step for the reaction since it the slowest step. The bond length of Mo=S was elongated by 0.18306Å which implies that the electron from substrate to enzyme was transferred through sulfido terminal. The dithiolate involve themselves by localization of electron density in the 'out of plane' sulfur-p_z orbitals in the presence of high electron density on the metal d_{xy} orbital and delocalize electrons by strong mixing with an empty in plane metal d_{xy} orbital when the electron density in the metal orbital is low, for oxidized Mo(VI). It was indicated by the study of fold angle of dithiolate that; *sp* orbitals of dithiolate serve as an essential instrument for buffering the electron density at the metal center [20].

The DFT calculation of this study for charge distribution of interactive carbon shows C2 position is more electrophilic relative to C8. In support of interactive site the study of sequential hydroxylation of hypoxanthine indicated that hypoxanthine is hydroxylated exclusively at the C2 position and C2 of hypoxanthine is comparably reactive as C8 of xanthine [18]. The negative charge accumulated on C6-S- of 6-MP or C6-O- of hypoxanthine during the transition state stabilized better through the interaction with the positively charged Arg_{880}.

For reaction mechanism the up conformers were selected depending on the minimum energy barrier they required for the transformation from reactant to product. Energy barrier observed in path II, III and IV were not observed in path I, therefore path II, III, and IV may be ruled out. Product formation showed very large exothermic energy values (-47222.09287kcal/mol and -47222.06107kcal/mol) for normalized energies of 6-MP and hypoxanthine respectively.

The calculated energy barrier between reactants (6-MP or hypoxanthine and active site) and substrate bound active site for path I was about 420.87kcal/mol which is so large. It is expected that the abstraction of proton from hydroxide ligand of active site by Glu_{1261} and simultaneous nucleophilic attack of hydroxo group of active site to electrophilic C2 of substrate coexist in the transition state (TS1). Hence the reaction may possess two transition states (TS1 and TS2). The second step is hydride transfer from substrate to sulfido terminal of active site with concomitant release of hydroxo ligand from active site to C2 of substrate takes place through TS2. Mullikan population of H_{RH} in the INT decreased by 0.095656 relative to reactant geometry, this implies the presence of a significant change of the charge density in TS1, which may support the presence of TS1.

Even if the most important feature for the enzymatic reaction considered is a hydride transfer from the substrate to the sulfido terminal of S_{Mo}, the barrier between TS1 and INT was expected to be implying that the reaction proceeds easily for hydride attack transition state TS2. The second transition state TS2 is the usual hydride transfer from substrate to sulfido terminal followed by release of hydroxylated product. From the, above hypothesis and data large due to proton abstraction, relatively the energy barrier between the INT and TS2 is about 2kcal/mol it can be concluded that the hydroxylation of 6-MP or hypoxanthine proceeds through stepwise mechanism as shown in Scheme 1.7. For the proposed reaction mechanism of formation of TS1 needs a careful optimization from reactant through TS1 to INT as it was done for calculation of TS2 including Glu_{1261} recommended. While the data is more consistent with a stepwise mechanism, the data presented herein does not exclude a concerted mechanism, and further experimental studies will be required to fully characterize the reaction.

References

1. Schwarz, G., (2005). Molybdenum cofactor biosynthesis and deficiency. Cell. Mol. *Life Sci., 62 (23), 2792 – 810.*
2. Kisker, C., Schindelin, H., Baas , D., Reètey , J., Meckenstock , R. U., andKroneck, P. M. (1999). A structural comparison of molybdenum cofactor-containing enzymes. FEMS Microbiology Reviews 22, 503 – 521.
3. Garattini, E., Mendel, R., Romao, M. J., Wright, R., and Terao, M., (2003). Mammalian molybdo-flavoenzymes, an expanding family of proteins: Structure, genetics, regulation, function and pathophysiology. Biochem. J., 372, 15 – 32.
4. Liu, M. T. W., Wuebbens, M. M., Rajagopalan, K. V., and Schindelin, H., (2000). Crystal Structure of the Gephyrin-related Molybdenum Cofactor Biosynthesis

Protein MogA from Escherichia coli. J Bio. Chem., (3), 1814 – 1822.
5. Mendel, R. R., (2007). Biology of the molybdenum cofactor. Journal of*Experimental Botany., 58 (9), 2289 – 2296.*
6. Rajagopalan, K. V., (1997). The molybdenum cofactors-perspective from crystalstructure. J Bio. Inorg. Chem., 2, 786 - 9.
7. Leimkuhler, S., Stockert, A. L., Igarashi, K., Nishino, T., and Hille, R. (2004). The role of active site glutamate residues in catalysis of Rhodobacter capsulatus xanthine dehydrogenase. J. Biol. Chem., 279, 40437 – 40444.
8. Amano, T., Ochi, N., Sato, H., and Sakaki, S., (2007). Oxidation reaction by xanthine oxidase: Theoretical study of reaction mechanism. J.Am. Chem. Soc. 129 (26), 8131- 8.
9. Nishino. T., Okamoto, K., Eger, B.T., and Pai, E. F., (2008). Mammalian xanthine oxidoreductase - mechanism of transition from xanthine dehydrogenase to xanthine oxidase. FEBS J., 275 (13), 3278 - 89.
10. Cho i, E. Y., Sto ckert, A. L., Leimkuhler, S., and Hille R., (2004). Studies on the mechanism of action of xanthine oxidase. J. Inorg. Biochem., 98 (5), 841 - 8.
11. Hille, R., (1997). Mechanistic aspects of the mononuclear molybdenum enzymes. *JBIC 2, 804 – 809.*
12. Okamoto, K., Matsumo to , K., Hille, R., E ger, B. T., Pai, E . F., and Nishino, T ., (2004). The crystal structure of xanthine oxidoreductase during catalysis: Implications for reaction mechanism and enzyme inhibition. Proc. Natl. Acad. *Sci.USA., 101, 7931 – 7936.*
13. Yamaguchi, Y., Matsumura, T., Ichida, K., Okamoto, K., and Nishino, T., (2007). Human Xanthine Oxidase changes its substrate specificity to Aldehyde Oxidase type upon mutation of amino acid residues in the active site: Roles of active site residues in binding and activation of purine substrate. J. Biochem., 141, 513 - 524.
14. Hernandez, B., Luque, F. J., and Orozco, M., (1996). Tautomerism of xanthine oxidase subs trates hypoxanthine and allop urinol. J. Org. Chem., 61, 5964 – 5971.
15. Enroth, C., Eger, B. T., Okamoto, K., Nishino, To., Nishino, Ta., and Pai, E. F., (2000). Crystal structures of bovine milk xanthine dehydrogenase and xanthine oxidase: Structure-based mechanism of conversion. Proc. Nat. Acad. Sci. USA., 97, 10723 – 10728.
16. Pauff ,J. M., Cao , H., and Hille, R., (2009). Substrate Orientation and Catalysis at the Molybdenum Site in Xanthine Oxidase: Crystal structures in complex with xanthine and lumazine. J. Bio.l Chem., 284 (13), 8760 - 7.
17. Kalra, S., Jena, G., Tikoo., and Mukhopadhyay, A. K., (2007). Preferential inhibition of xanthine oxidase by 2-amino-6-hydroxy-8-mercaptopurine and 2-amino-6-purine thiol. BMC Biochemistry., 8(8), 1 - 11.
18. Cao, H., Pauff1, J. M., and Hille, R., (2010). Substrate orientation and catalytic specificity in the action of xanthine oxidase: The sequential hydroxylation of hypoxanthine to uric acid. J. Biol. Chem., Papers in Press page 1 - 23.
19. Zhang, X. H., and Wu, Y. D., (2005). A theoretical study on the mechanism of the reductive half-reaction of xanthine oxidase. Inorg.Chem., 44 (5), 4416 - 1471.
20. Joshi, H. K., Cooney, J. J. A., Inscore, F. E., Gruhn, N. E., Lichtenberger, D L., and Enemark, J. H., (2003). Investigations of metal–dithiolate fold angle effects: Implications for molybdenum and tungsten enzymes. PNAS., 100 (7) 3719 – 3724.
21. Sabiah, S., and Viswanathan., (2009). Mo-amino acid complexes as analogs for molybdoenzyme: A DFT approach. Indian Journal of Chemistry., 48 (A), 911 - 920.
22. Nishino, T., Okamoto, K., Eger, B. T., Pai, E. F., and Nishino, T., (2008). Mammalian xanthine o xidored uctase: Mechanis m of transition from xanthine dehydrogenase to xanthine oxidase. Review Article., 275, 3278 – 3289.